

Thermal Conductivity, Electrical Resistivity, and Seebeck Coefficient of Silicon from 100 to 1300°K†

W. FULKERSON, J. P. MOORE, R. K. WILLIAMS, R. S. GRAVES, AND D. L. MCELROY
Metals and Ceramics Division, Oak Ridge National Laboratory, Oak Ridge, Tennessee

(Received 2 August 1967)

Results are presented of measurements of the thermal conductivity (90–1328°K), the electrical resistivity (300–1273°K), and the Seebeck coefficient (350–1273°K) for single-crystal and large-grained polycrystalline specimens of 99.99+% pure silicon. The thermal conductivity above 387°K was measured by an absolute radial-heat-flow technique; below 350°K, by an absolute longitudinal technique. Some intermediate thermal-conductivity measurements from 300–400°K were made on the polycrystalline material using a comparative longitudinal-heat-flow apparatus. The estimated errors of these three thermal-conductivity methods were $\pm 2\% \pm 2^\circ\text{K}$, $\pm 1.2\% \pm 0.1^\circ\text{K}$, and $\pm 4.0\% \pm 1^\circ\text{K}$, respectively. The estimated error for the electrical-resistivity measurements was $\pm 1.4\% \pm 2^\circ\text{K}$, and for the Seebeck measurements $\pm 1.6\% \pm 2^\circ\text{K}$. The thermal-conductivity values were compared with conflicting data from the literature, and they corroborate the higher-temperature results obtained by Glassbrenner and Slack. Therefore, we agree with their conclusion that the electronic contribution is reasonably close to theoretical estimates which include a large ambipolar-diffusion term. The temperature dependence of the lattice thermal resistance has been compared to various theoretical models but no approach seems to explain the data in detail. An abrupt slope change in the thermal resistivity at about 670°K is a major cause of the difficulty.

INTRODUCTION

RECENT studies of the thermal conductivity k , of silicon by Glassbrenner and Slack¹ and by Shanks, Maycock, Sidles, and Danielson² disagree about the high-temperature behavior. Shanks *et al.* found k to decrease with temperature to an approximately constant value above 1050°K, whereas Glassbrenner and Slack found that k continued to decrease albeit at a slower rate than at lower temperatures. On the basis of the electrical-resistivity and carrier-mobility data of Morin and Maita,³ Glassbrenner and Slack calculated the electronic contribution to the thermal conductivity. They found reasonable agreement with “experimental” values obtained by extrapolating the thermal-resistivity temperature dependence from low temperatures where the electronic contribution was negligible.

Shanks *et al.* also used the mobility values of Morin and Maita, but they measured the electrical resistivity of their own specimen which they found to be a factor of 2 greater than that obtained by Morin and Maita for intrinsic silicon. With this higher resistivity and using the same equation for the ambipolar contribution, they calculate an electronic contribution which is about twice that reported by Glassbrenner and Slack. This calculation is in error by about a factor of 4 considering the electrical resistivity values of Shanks *et al.* If the lattice portion of the thermal conductivity decreases as $1/T$ and if this relation can be extrapolated from lower temperatures, the electronic portion of k obtained from the data of Shanks *et al.* is much greater than predicted by the ambipolar theory used by both sets of authors.

More recent measurements by Klein, Shanks, and

Danielson⁴ at the Ames Laboratory on the same specimens measured by Shanks *et al.*³ are in much better agreement with the data of Morin and Maita; furthermore, the electronic component to the thermal conductivity was recalculated by Klein *et al.*⁴ and agrees with the calculation of Glassbrenner and Slack.

The disagreement in the published high-temperature thermal-conductivity results prompted us to repeat the measurements on silicon. We also decided to measure the electrical resistivity and Seebeck coefficient of our specimen, because of the disagreement between Shanks *et al.* and Morin and Maita.

SPECIMEN CHARACTERIZATION AND PREPARATION

Two single-crystal disks and eight polycrystalline disks of silicon were procured from Semi-Elements, Inc.,⁵ and were stated to have impurity concentrations less than 20 parts per million (ppm) total. This disks were 5.07 cm in diam by 2.54 cm thick. The bulk densities of the disks obtained from the measured volume and weight were 2.327 and 2.326 g/cm³ for the single-crystal and polycrystalline disks, respectively, at room temperature. The theoretical density calculated from lattice parameters was 2.333 g/cm³. Our experimental densities agree well with a value of 2.329 reported by Smakula, Kalnajs, and Sils.⁶ Table I shows the results of chemical analyses indicating that the impurity contents were 27 and 55 ppm for the single-crystal and polycrystalline specimens, respectively. These analyses were made on material cut from the spiral radial-heat-flow measuring disks described below. Specimens for electrical-resistivity–Seebeck-coefficient measurements

† Research sponsored by the U. S. Atomic Energy Commission under contract with the Union Carbide Corporation.

¹ C. J. Glassbrenner and Glen A. Slack, *Phys. Rev.* **134**, A1058 (1964).

² H. R. Shanks, P. D. Maycock, P. H. Sidles, and G. C. Danielson, *Phys. Rev.* **130**, 1743 (1963).

³ F. J. Morin and J. P. Maita, *Phys. Rev.* **94**, 1525 (1954).

⁴ A. H. Klein, H. R. Shanks, and G. C. Danielson, in *Proceedings of the Third Conference on Thermal Conductivity*, Gatlinburg, Tennessee, 1963 (unpublished).

⁵ Semi-Elements, Inc., Saxtonburg, Pa.

⁶ A. Smakula, J. Kalnajs, and V. Sils, *Phys. Rev.* **99**, 1744 (1955).

TABLE I. Chemical analysis results on silicon.

Element	Single crystal (ppm)	Polycrystal (ppm)
	Semiquantitative ^a	
Ag	<0.04	<0.7
B	<0.005	<0.07
Be		<1.0
Ca	0.02	<0.2
Nb	<0.03	<0.3
Cr	<0.1	0.3
Fe	<0.1	<4.0
K	<0.1	<0.1
Mg	<1.0	<1.0
Mn	<0.05	<0.2
P	<0.3	12.0
Ta	<0.7	<0.7
Th	<1.0	<0.3
Ti	<1.0	<0.3
	Quantitative ^b	
Cu	0.018, 0.034	0.14, 0.093
Na	0.21, 0.23	0.79, 0.57
U	0.15	0.054
W	0.010, 0.065	0.102, 0.072
H ₂	3	4
O ₂	14	24
N ₂	5	5
Total (maximum)	26.9	55.3

^a The values reported should be within a factor of 2 of the actual value; semiquantitative values were obtained by mass spectroscopy.

^b The quantitative analysis of Cu, Na, U, and W were by neutron activation and the two values reported for Cu, Na, and W were taken on different parts of the specimen indicating impurity-concentration inhomogeneity.

and for metallographic examination were cut from this same material. Naturally, some variation in impurity content from disk to disk is expected and the higher impurity content of the polycrystalline disk should not be interpreted as meaning that all eight polycrystalline disks had a larger impurity content than the single-crystal specimen. The analyses only indicate the order of magnitude of the impurities in the disks. The room-temperature electrical resistivities were 140 and 36 Ω cm for the single-crystal and polycrystalline materials, respectively. This indicates that the relative impurity contents of the two materials are as shown in Table I.

Two specimens were examined metallographically and suitable etching revealed an etch-pit density of 2.0×10^4 and $6.0 \times 10^4/\text{cm}^2$ for the poly- and single-crystal specimens. This etch-pit density is believed to be indicative of dislocation density.⁷ The etched specimens gave no indication of grain boundaries or inclusions. Laue x-ray patterns taken at various points across the surface of the specimens confirmed the single-crystal state, and small-angle x-ray measurements revealed no subgrain structure. This was true for the polycrystal as well as the single-crystal specimen, and led to the conclusion that the polycrystalline specimens were extremely coarse grained (grains of the order of 1 cm or more on a side). From the point of view of the transport properties reported in this paper there was no difference between the polycrystalline and the single-crystal specimens, and these designations are used only for identification.

⁷ W. C. Dash, J. Appl. Phys. **29**, 736 (1958); **30**, 459 (1959); **31**, 736 (1960).

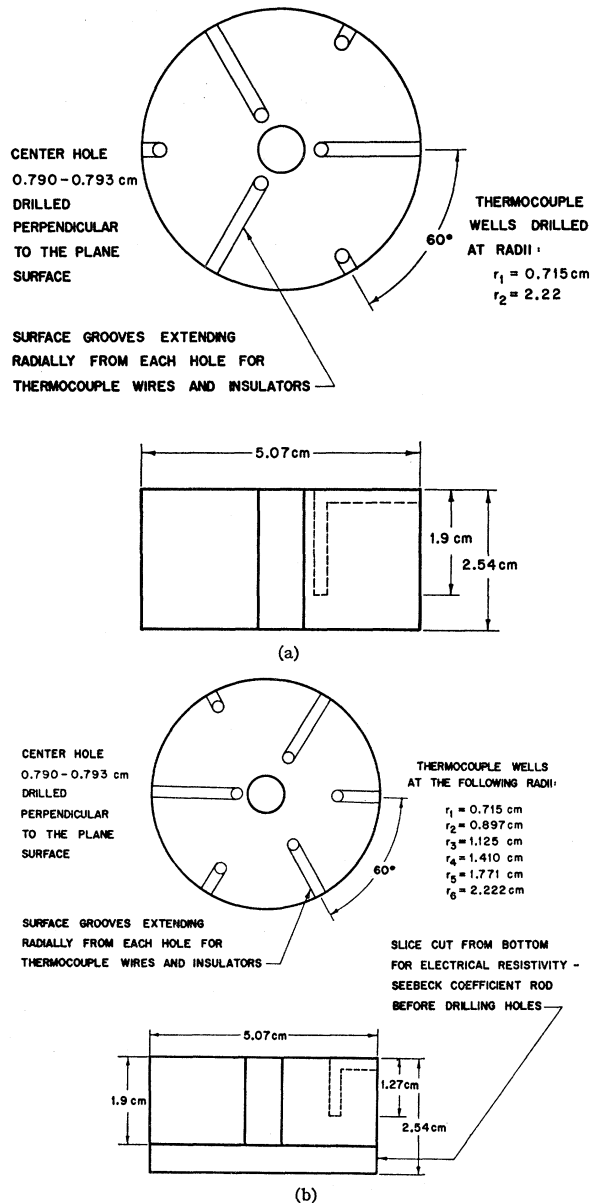


FIG. 1. Radial-heat-flow measuring planes. (a) Regular plane. (b) Spiral plane.

Nine of the ten disks were used in the radial-heat-flow thermal-conductivity apparatus, but only four were instrumented with thermocouples. Of these, one single-crystal and one polycrystalline disk were machined as shown in Fig. 1(a) and are called regular planes. The wells in these disks were 0.159 cm in diam and 1.905 cm deep. The two other instrumented disks (one polycrystal and one single crystal) were machined as shown in Fig. 1(b) and are called spiral planes. A 0.633-cm slice was cut from the bottom of each of the two spiral disks for material to make resistivity specimens, chemical analyses, and microstructure determinations as mentioned above. As a consequence of taking

TABLE II. Particulars for the five assemblies of the radial-heat-flow apparatus.

Assembly	Measuring planes	Thermocouples	Maximum temperature (°K)	Number of data points
1	Regular single crystal	(Pt-10% Rh)-Pt	793	33
	Spiral single crystal	(Pt-10% Rh)-Pt		
2	Regular polycrystal	(Pt-10% Rh)-Pt	770	10
	Spiral polycrystal	(Pt-10% Rh)-Pt		
3	Regular polycrystal	(Pt-10% Rh)-Pt	1198	21
	Spiral single crystal	(Pt-10% Rh)-Pt		
4	Regular single crystal	(Pt-10% Rh)-Pt	1328	20
	Regular polycrystal	(W-5% Re)-(W-26% Re)		
5	Regular single crystal	(Pt-10% Rh)-Pt	782	15
	Regular polycrystal	(Pt-10% Rh)-Pt		

this slice the thermocouple wells were drilled 1.27 cm deep rather than 1.905 cm for the regular planes.

Two resistivity specimens were machined, one from the slice off the polycrystalline spiral disk and the other from the slice off the single-crystal spiral disk. The resistivity specimens were rods 5.07 cm long cut with a square cross section approximately 0.381 cm on a side. The specimens were ground so that opposite sides were flat and parallel. Two 0.056-cm-diam holes 2.0 cm apart were drilled through the polycrystalline specimen for the insertion of thermocouples. Each hole was approximately 1.525 cm from an end of the rod.

From the tenth polycrystalline disk the comparative longitudinal-heat-flow specimen was machined. This specimen was a right circular cylinder 2.11 cm high by 1.27 cm in diam. The ends were lapped flat to $\frac{1}{2}$ fringe and parallel to within 0.0025 cm.

APPARATUS AND EXPERIMENTAL ERRORS

Radial-Heat-Flow Thermal-Conductivity Apparatus

The thermal-conductivity measurements to high temperatures were made using the Oak Ridge National Laboratory (ORNL) radial-heat-flow apparatus which has been described extensively in the literature (McElroy *et al.*⁸ and Godfrey *et al.*⁹). This apparatus has yielded accurate absolute measurements to above 1300°K¹⁰ on a number of materials including UO₂ (Godfrey *et al.*¹¹) and Armco iron (Fulkerson *et al.*¹²) which is considered a thermal-conductivity reference standard. The only major change made in the apparatus for this study was the use of a 0.61-cm-diam carbon-rod

core heater to replace a wire-wound core heater. This permitted a higher power density with available power supplies and reduced the necessary size of the central hole in the specimen so that smaller diameter specimens could be measured to the same accuracy. Three voltage taps made from 0.0127-cm-diam W-26% Re wire were attached to the core heater in the central 7.6 cm where the measuring planes were located. These taps were attached by twisting tight a loop of the wire around the core heater into a 0.0178-0.0254-cm groove machined in the carbon rod. The wires passed radially out of the specimen stack through grooves machined in the disks and were insulated from the specimen by single-hole 0.158-cm-diam Al-23 Degussit¹³ alumina tubing. Three voltage taps rather than two gave the advantage that the core-heater power could be checked for longitudinal uniformity. Also, there was a spare tap if one broke during a measurement, which happened during assembly 3.

The radial-heat-flow measurements consisted of five separate assemblies of the apparatus and resulted in 99 data points between 387 and 1328°K. For each assembly the specimen stack was completely reinstrumented with new thermocouples. All except the tenth silicon disk were in the apparatus during each assembly but only two of the four measuring planes were instrumented at a time. Table II gives some of the particulars for each assembly. Reference-grade annealed Sigmund-Cohn¹⁴ 0.0254-cm-diam (Pt-10% Rh)-Pt thermocouples were used throughout except for the regular polycrystal plane during assembly 4 for which 0.0254-cm-diam (W-5% Re)-(W-26% Re) thermocouples from Hoskins¹⁵ were used. Direct contact of the platinum-rhodium thermocouple measuring junctions and the silicon was prevented by small alumina spacer tubes at the bottom of each thermocouple well.⁹ The tungsten-rhenium thermocouple measuring junctions were allowed to touch the silicon.

The thermal conductivity was calculated for the

⁸ D. L. McElroy, T. G. Godfrey, and T. G. Kollie, *Trans. Am. Soc. Metals* **55**, 749 (1962).

⁹ T. G. Godfrey, W. Fulkerson, T. G. Kollie, J. P. Moore, and D. L. McElroy, Oak Ridge National Laboratory Report No. ORNL-3556, 1964 (unpublished).

¹⁰ Our experience with our radial-heat-flow apparatus has been that we can push the equipment well above 1273°K but we run into thermocouple-instability problems at higher temperatures. The highest temperature at which we were able to obtain reliable data in the case of silicon was 1328°K.

¹¹ T. G. Godfrey, W. Fulkerson, T. G. Kollie, J. P. Moore, and D. L. McElroy, *J. Am. Ceram. Soc.* **48**, 297 (1965).

¹² W. Fulkerson, J. P. Moore, and D. L. McElroy, *J. Appl. Phys.* **37**, 2639 (1966).

¹³ Degussit Division of Degussa, Inc., Kearny, N. J.

¹⁴ Sigmund-Cohn Corporation, Mt. Vernon, N. Y.

¹⁵ Hoskins Manufacturing Co., Detroit, Mich.

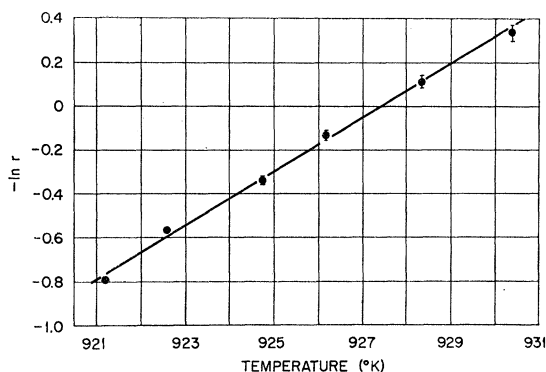


FIG. 2. A typical temperature profile for the single-crystal spiral disk at 926°K.

spiral planes from the formula

$$k = \frac{-Q}{2\pi l} \frac{d(\ln r)}{dt}, \quad (1)$$

where the slope $d(\ln r)/dt$ was obtained from a least-squares fit of the values of $\ln r$ versus t . The emf reading for each thermocouple was corrected by the usual isothermal intercomparison of all the thermocouples at the same temperature, a procedure described by Godfrey *et al.*⁹ Figure 2 shows a plot of $\ln r$ versus t for a typical data point at 926°K. The bands around the points indicate the uncertainty in the radial position of the thermocouples. The least-squares line lies outside the error bands around three of the points. This may be due to temperature-measurement errors not corrected by the isothermal intercomparison, such as might arise from inhomogeneities in the thermocouple wire along the radial grooves of the specimen, or it may be due to asymmetric radial heat flow. The reason for using the spiral arrangement of thermocouples was to detect possible thermal-radiation-transmission effects which would make the inside and outside thermocouples read significantly off the straight line. No such effects were detected outside the scatter shown in Fig. 2. At the temperature of the data shown in Fig. 2, radiation transmission is insignificant, as is shown in the discussion below.

For all of the assemblies the measured thermal conductivity of the spiral planes was 1–4% lower than the results for the regular planes. The two spiral planes agreed well with each other as did the two regular planes. This apparent nonrandom difference between the types of planes was probably due to real specimen differences, since specimen changes of this order of magnitude were observed to result from heat treatment. Both types of planes gave essentially the same temperature dependence of k .

Another problem with the radial thermal-conductivity results was that the values obtained for the polycrystalline regular plane during assembly 4 using the (W–5% Re)–(W–26% Re) thermocouples were initially 4–5% higher than those obtained using (Pt–10% Rh)–Pt

thermocouples for the same plane for assemblies 2 and 3. During the initial heat up for assembly 4 the results for the (W–5% Re)–(W–26% Re)-instrumented plane approached those obtained for the same plane during the previous assemblies. At 972°K the results were in agreement within 1%. This gradual change with temperature can probably be attributed to annealing of the W–5% Re and W–26% Re wire. However, on heating above 972°K two of the six (W–5% Re)–(W–26% Re) thermocouples broke. This caused a shift in the data obtained during the rest of assembly 4, so that the results remained 4–5% away from the platinum-rhodium values obtained previously on this disk. This shift was entirely due to the loss of the two thermocouples since a recalculation of the data point at 972°K using only the four thermocouples which survived led to a shift of that data point in agreement with subsequent data obtained after the two thermocouples failed. However, the same temperature dependence was obtained after the shift for both types of thermocouples, which was the important part of the experiment since the (W–5% Re)–(W–26% Re) were used to verify the high-temperature behavior observed using the (Pt–10% Rh)–Pt thermocouples.

Absolute Longitudinal-Heat-Flow Apparatus

Thermal-conductivity measurements in the range 78–350°K were made with an absolute longitudinal-heat-flow apparatus using the polycrystalline electrical-resistivity specimen after the electrical-resistivity measurements to 1273°K had been completed. A heater was wound on one end of the specimen and the other end was attached to a heat sink connected by a controllable thermal resistance to the cryostat. Two Chromel-Constantan thermocouples in the 0.056-cm-diam holes in the specimen were used to determine the temperature gradient. The specimen was surrounded by a guard cylinder to reduce heat exchanges by conduction down the thermocouple and heater lead wires, and a thin film of gold was applied to the specimen surface to reduce radiation exchange. Radiation exchange was further reduced by filling the annulus between the specimen and the guard cylinder with Fiberfrax.¹⁶ The measurements were carried out in a vacuum of about 10^{-6} Torr to eliminate gaseous conduction. A detailed description of the apparatus and experimental procedure is reported elsewhere by Moore *et al.*¹⁷

Comparative Longitudinal-Heat-Flow Apparatus

Thermal-conductivity measurements between 300 and 400°K were made using a technique which is de-

¹⁶Fiberfrax alumina and silica fibers from the Carborundum Company, Refractories and Electronics Division, Niagara Falls, N. Y.

¹⁷J. P. Moore, D. L. McElroy, and R. S. Graves, *Can. J. Phys.* **45**, 3849 (1967).

scribed in detail by Moore *et al.*¹⁸ on a polycrystalline silicon specimen cut from the tenth unheated disk. The method consists of pressing the unknown specimen between two bars of iron of known thermal conductivity. The temperature gradients are measured in the iron bars to obtain the heat flow and temperature drop across the specimen, and hence the thermal conductivity can be determined. The test is performed in vacuum to minimize heat losses, and the test has the advantage that the specimen does not have to be instrumented with thermocouples. This technique was employed primarily to study the effects of various heat treatments on small silicon samples.

Electrical-Resistivity-Seebeck-Coefficient Apparatus

Measurements of the electrical resistivity and Seebeck coefficient of polycrystalline and single-crystal specimens were made to 1273°K in a vacuum of 10^{-6} – 10^{-7} Torr or under a helium atmosphere at temperatures below 873°K. The helium served to provide good thermal contact between the specimen and the thermocouples during the Seebeck measurements below 873°K. Above this temperature Seebeck measurements in He and in vacuum agreed, presumably because of increased radiation heat transfer at high temperatures. The electrical-resistivity measurements were the same in vacuum and in He at all temperatures. Most of the details of the apparatus are described elsewhere¹²; however, the instrumentation of each specimen was different. Tantalum voltage taps and (W-5% Re)-(W-26% Re) thermocouples were wired onto the single-crystal specimen. The thermocouples were made by wrapping 0.013-cm-diam W-5% Re wire around the ends of 0.025-cm-diam W-5% Re and W-26% Re thermocouple wires. This wrapped junction was pressed against the side of the specimen. The tantalum voltage taps were also pressed against the side of the specimen with a separation of 2 cm. Tantalum wire twisted around each end of the specimen served as the current leads for the four-probe resistivity technique. The distance between voltage taps was determined by a traveling stage microscope. This distance was checked before run 1 and after run 4 and was found to have changed by 1.4%. The instrumentation of the polycrystalline specimen was better and more simple since the wrapping of the thermocouples and voltage taps to the specimen was avoided. Instead, 0.025-cm-diam W-(W-26% Re) thermocouple wires were pressed into 0.056-cm-diam holes drilled in the specimen, to yield a thermocouple junction in good thermal contact with the specimen. The tungsten wires of the thermocouples were used as voltage taps, and the distance between the taps was determined electrically by comparison to a standard knife edge at room temperature. Tantalum current leads were used. Despite the difference in instrumentation, the

electrical-resistivity measurements in the intrinsic range for both specimens agreed to within $\pm 2\%$.

The various thermocouple, current, and voltage tap leads were insulated by Al 23 Degussit alumina tubing. The current for the measurement of electrical resistivity was of the order of 1.5 mA and was supplied by a Kepco¹⁹ dc power supply, model ABC 425M, operating in the constant-current mode. This constant-current capability was very useful since the contact resistance between the tantalum current leads and the specimen was generally very high and considerably different for the two directions of current flow because of rectification.

The W-(W-26% Re) and (W-5% Re)-(W-26% Re) thermocouples were calibrated by comparison to a (Pt-10% Rh)-Pt thermocouple, and from this calibration corrections were obtained for the smoothed Hoskins thermocouple tables of Adams and Davisson.²⁰ The same corrections were applied to the radial-heat-flow data taken for the regular polycrystalline disk during assembly 4.

Measurement Errors

Table III summarizes the estimated determinate and indeterminate errors in measurements of the thermal conductivity, electrical resistivity, and Seebeck coefficient. The determinate errors are the uncertainties in the measurements required to determine the result. These include, for example, the potentiometer errors in reading thermocouple emf's and voltage drops but not errors in thermocouple calibration or difficulties in the thermocouple system that cause an incorrect thermal emf. The latter errors are designated indeterminate.

We have assigned an arbitrary $\pm 2^\circ\text{K}$ uncertainty in the temperature measurements above room temperature [1°K to account for inherent inaccuracies in the thermocouple tables and 1°K for the divergence of our (Pt-10% Rh)-Pt thermocouples from the values given in the tables]. This assigned temperature error is probably excessive especially below about 873°K; however, we have drawn attention to this error to make the reader aware of the fact that each data point as plotted on a graph has an uncertainty in both the abscissa as well as the ordinate.

The indeterminate error for the Seebeck coefficient associated with the transverse temperature gradient on the thermocouple hot junctions was calculated assuming that this gradient was the same as that along the specimen during the measurement.¹² The error arises because of the physical dimensions of the hot junction which results in the possibility that the Seebeck voltage is measured at one position (the effective electrical point of contact of the thermocouple wires with the specimen) but the thermocouple reads a temperature at a point at least a wire diameter removed from the electrical

¹⁸ J. P. Moore, R. S. Graves, T. G. Kollie, and D. L. McElroy, Oak Ridge National Laboratory Report No. ORNL-4121, 1967 (unpublished).

¹⁹ Kepco, Inc., Flushing, N. Y.

²⁰ R. K. Adams and E. G. Davisson, Oak Ridge National Laboratory Report No. ORNL-3649, Vol. 2, 1965 (unpublished).

TABLE III. Summary of errors associated with the thermal-conductivity, electrical-resistivity, and Seebeck-coefficient measurements.

Error	Thermal conductivity			Electrical resistivity	Seebeck coefficient	
	Radial heat flow (regular plane)	Absolute longitudinal heat flow	Comparative longitudinal heat flow			
		Determinate				
Power measurement ^a	0.4%	±0.37%	±2.7%			
Thermocouple position	3.1% (inside) 1.0% (outside)	±0.36%				
Thermocouple reading (temperature gradient)	0.2%	±1.0%	±3.1%		0.3%	
Voltage reading				0.02%		
Current reading				0.12%		
Area		±0.13%	±0.08%	0.2%		
Length between voltage taps				0.1%		
Thermocouple Seebeck coefficient	0.5%				0.5%	
Total determinate	5.3%	1.86%	5.88%	0.44%	0.93%	
Most probable ^b	~2.0%	±1.2%	±4.0%	~0.3%	~0.6%	
		Indeterminate				
Temperature	±2°K	±0.1°K	±1°K	±2°K	±2°K	
Transverse gradient on the thermocouple hot junction					4% (single crystal) 1% (polycrystal)	
Voltage tap position shift				±1.4% (single crystal)		
Total	±2.0%±2°K	±1.2%±0.1°K	±4.0%±1°K	±1.7%±2°K (single crystal) ±0.3%±2°K (polycrystal)	±4.6%±2°K (single crystal) ±1.6%±2°K (polycrystal)	

^a Including voltage tap location.

^b The most probable error is defined as $(\sum \epsilon_i^2)^{1/2}$, where ϵ_i are the errors associated with the individual measurements. The value for the thermal conductivity by the radial-heat-flow technique for a regular plane is calculated assuming that the three inside thermocouples and the three outside thermocouples are equivalent. [T. G. Godfrey *et al.*, Oak Ridge National Laboratory Report No. ORNL-3556, 1964 (unpublished).]

contact point with the specimen. The error can be much larger than that calculated if the thermal contact of the hot junction to the specimen is poor. This is easily demonstrated by measuring the Seebeck coefficient in a vacuum and then in helium. At low temperatures the results are often very different. Above approximately 873°K thermal radiation provides good thermal contact between the hot junction and the specimen, and the helium and vacuum measurements agree.

EXPERIMENTAL RESULTS

Thermal Conductivity

Throughout most of this paper we have found it convenient to discuss the temperature behavior of thermal resistivity $1/k = W$ rather than thermal conductivity itself. Empirically, we found that over wide ranges of temperature the thermal-resistivity data could be fitted well to linear equations. Figure 3 shows the over-all temperature behavior of the thermal-resistivity data which is linear from about 130 to about 670°K. Between 650 and 690°K there is a slope change and then the data again has a linear behavior to about 1050°K above which the resistivity curves downward away from the straight line. This deviation is indicative of the increasing importance of an electronic contribution to the thermal conductivity. Below 130°K the data begin to swing up indicating the proximity of the low-temperature maximum in the thermal conductivity. The agreement of the

data obtained by the various methods of measurement is shown in Fig. 4. It is seen that the agreement is generally within the combined determinate experimental error of the techniques.

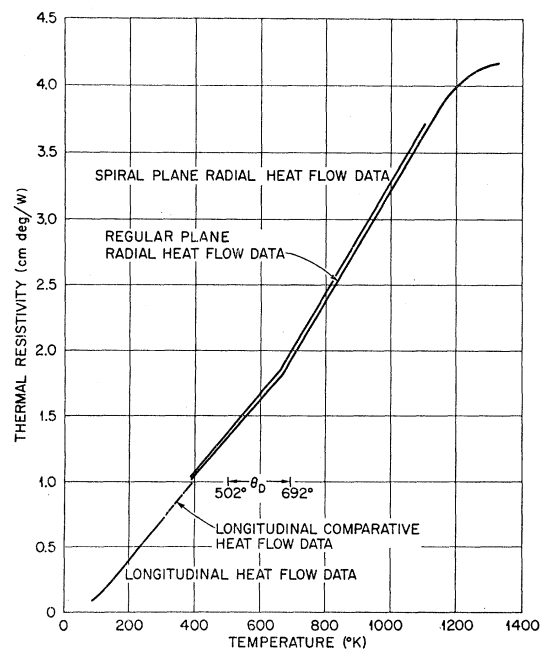


FIG. 3. The temperature behavior of the thermal resistivity of silicon indicated by ORNL data.

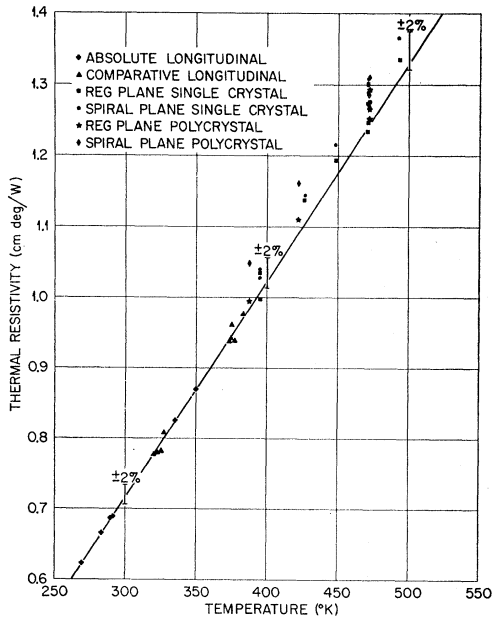


FIG. 4. Comparison of ORNL thermal-resistivity data for silicon taken by the radial-heat-flow, the absolute longitudinal-heat-flow, and the comparative longitudinal-heat-flow apparatus.

Besides the high-temperature deviation from linearity, the change in slope at about 670°K is the most singular characteristic of the thermal resistivity for silicon. This behavior is magnified in Figs. 5 and 6, where the data for the regular single-crystal plane obtained during

assembly 1 and for both single-crystal and polycrystal regular planes during assembly 5 are plotted, respectively. The data were taken at about 15°K intervals through the region of the slope change and the points are numbered to indicate chronology. Figure 5 shows that the thermal resistivity of the regular single-crystal disk increased about 0.04 cm deg/W during the initial heating of this specimen. This is indicated by the fact that points 1 and 2 are low whereas point 3 is on the line and in agreement with the rest of the points. We do not know the cause of this initial shift in resistivity. Although we have pointed out that the data for any particular plane and assembly have a probable error of $\pm 2\%$, one can see from Figs. 5 and 6 that the data for any given plane have very little scatter. For this reason we believe that the temperature dependence of the thermal resistivity is given more precisely by the data for a single plane during a particular assembly than by the average of the data for several assemblies. The change in slope at about 670°K was a universal observation for all of the planes in all of the assemblies and the cause for this break needs to be uncovered.

Table IV gives smoothed values for the thermal conductivity and thermal resistivity. These were obtained by the following methods:

(a) $100 \leq T \leq 350^\circ\text{K}$: from a smooth curve through the absolute longitudinal-heat-flow data;

(b) $400 \leq T \leq 650^\circ\text{K}$: from a least-squares fit of the radial-heat-flow data below 670°K to a linear equation $1/k = -0.1171 + 2.954 \times 10^{-3}T$;

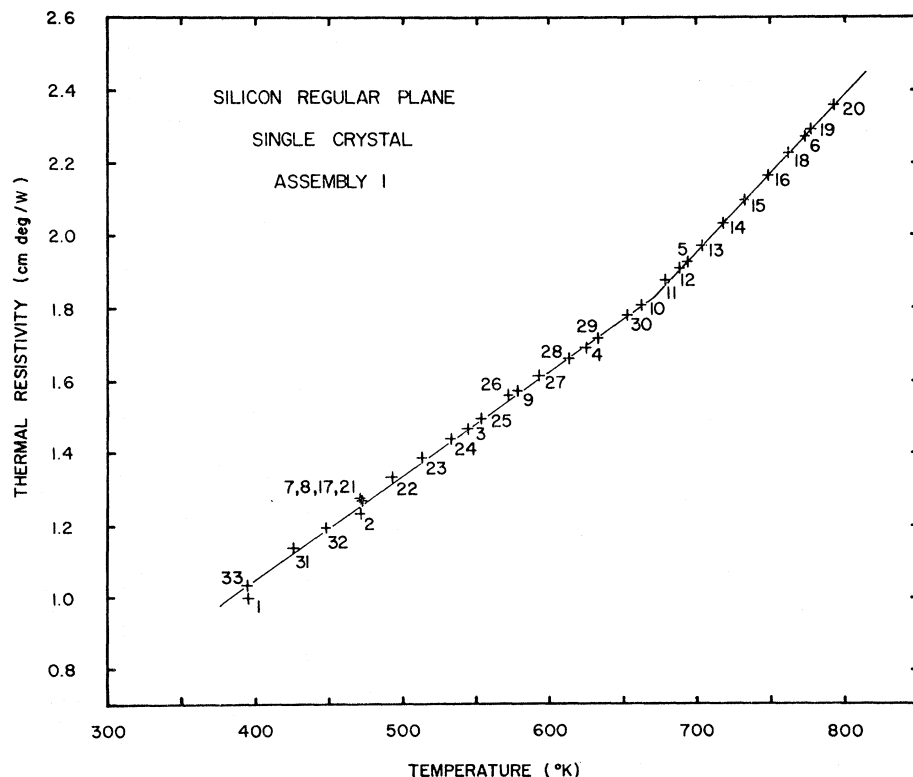


FIG. 5. Thermal-resistivity data for the regular single-crystal plane during assembly 1.

TABLE IV. Smoothed data for the thermal conductivity and thermal resistivity of silicon.

T (°K)	Smoothed ORNL Values		Shanks <i>et al.</i> ^a		Glassbrenner and Slack ^b	
	k (W cm ⁻¹ deg ⁻¹)	$W=1/k$ (cm deg W ⁻¹)	W (cm deg W ⁻¹)	Percent deviation	W (cm deg W ⁻¹)	Percent deviation ^c
100	7.52	0.133			0.105	-21
150	3.88	0.258				
200	2.44	0.410			0.375	- 8.5
250	1.78	0.563				
300	1.40	0.716	0.707	- 1.3	0.640	-10.5
350	1.15	0.870				
400	0.939	1.065	1.03	- 3.3	0.950	-10.7
450	0.825	1.212				
500	0.736	1.359	1.445	6.3	1.25	- 8.0
550	0.663	1.508				
600	0.604	1.656	1.735	4.8	1.56	- 5.8
650	0.555	1.803				
700	0.500	1.999	2.07	3.5	1.92	- 3.9
750	0.452	2.210				
800	0.413	2.420	2.50	3.3	2.33	- 3.7
850	0.380	2.634				
900	0.351	2.845	2.97	4.4	2.74	- 3.7
950	0.327	3.055				
1000	0.306	3.268	3.355	2.7	3.23	- 1.2
1050	0.287	3.479				
1100	0.273	3.657	3.45	- 5.7	3.57	- 2.5
1150	0.261	3.82 ₉				
1200	0.251	3.97 ₇	3.46	-13.1	3.83	- 3.8
1250	0.245	4.08 ₁				
1300	0.241	4.14 ₉	3.475	-14.9	4.04	- 2.7
1350	0.239	4.18 ₉				

^a H. R. Shanks, P. D. Maycock, P. H. Sidles, and G. C. Danielson, Phys. Rev. 130, 1743 (1963).

^b C. J. Glassbrenner and Glen A. Slack, Phys. Rev. 134, A1058 (1964).

^c Percent deviation is equal to [(study-ORNL)/ORNL] × 100.

(c) $700 \leq T \leq 1050^\circ\text{K}$: from a least-squares fit of the radial-heat-flow data in the range $670 \leq T \leq 1050^\circ\text{K}$ to a linear equation $1/k = -0.9609 + 4.229 \times 10^{-3}T$;

(d) $1100 \leq T \leq 1350^\circ\text{K}$: from a smooth curve through the regular single-crystal-plane radial-heat-flow data of assembly 4.

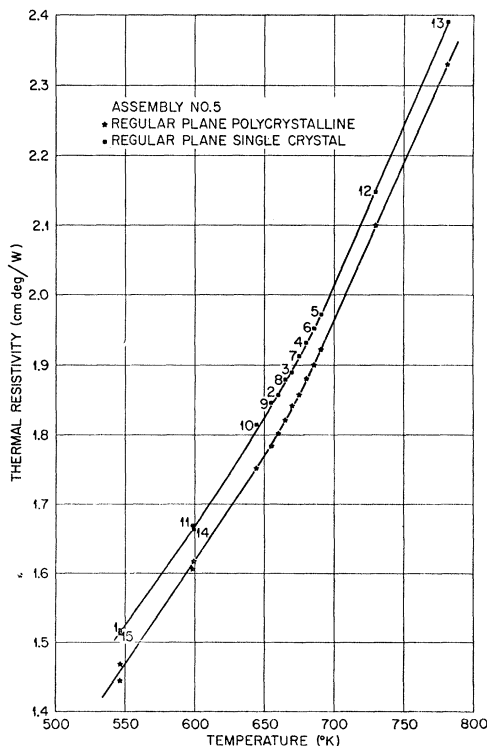


FIG. 6. Radial-heat-flow data taken during assembly 5 showing the break in the thermal-resistivity curve.

Also given in Table IV are the smoothed thermal-resistivity values of Glassbrenner and Slack¹ and of Shanks *et al.*² and the percentage deviation of these results from our smoothed values. This deviation is plotted in Fig. 7 along with the deviations of the results of several other investigators tabulated in the TPRC Data Books.²¹ We agree to within the combined experimental errors of the determinations with the values reported by Shanks *et al.*² up to 1000°K above which temperature the two sets of data diverge rapidly. The agreement between our data and those of Glassbrenner and Slack¹ is within combined experimental error ($\pm 7\%$) above 550°K and is in excellent agreement above 700°K (4% or better). Thus the major purpose of the investigation—to discriminate between conflicting data at high temperature—has been fulfilled, and the high-tempera-

²¹ The TPRC Data Books (unpublished) are a compilation of physical property data obtainable from the Thermophysical Properties Research Center at Purdue University. From these volumes we obtained the values plotted in Fig. 7: TPRC recommended values; P. V. Gel'd, Zh. Tekhn. Fiz. 27, 113 (1957) [English transl.: Soviet Phys.—Tech. Phys. 2, 95 (1957)]; Audrey D. Stukes, Phil. Mag. 5, 84 (1960); R. Bobone, L. F. Kendall, and R. H. Vought, TCREC Technical Report No. 62-112, p. 11, 1963 (unpublished); M. G. Holland, in *Proceedings of the Seventh International Conference on Low-Temperature Physics, Toronto, 1960* (University of Toronto Press, Toronto, 1961), pp. 280–284. We obtained the values of D. S. Beers, G. D. Cody, and B. Abeles [in *Proceedings of the International Conference on the Physics of Semiconductors, Exeter, 1962* (Institute of Physics and the Physical Society, London, 1962), pp. 41–48] from Fig. 1 of their paper.

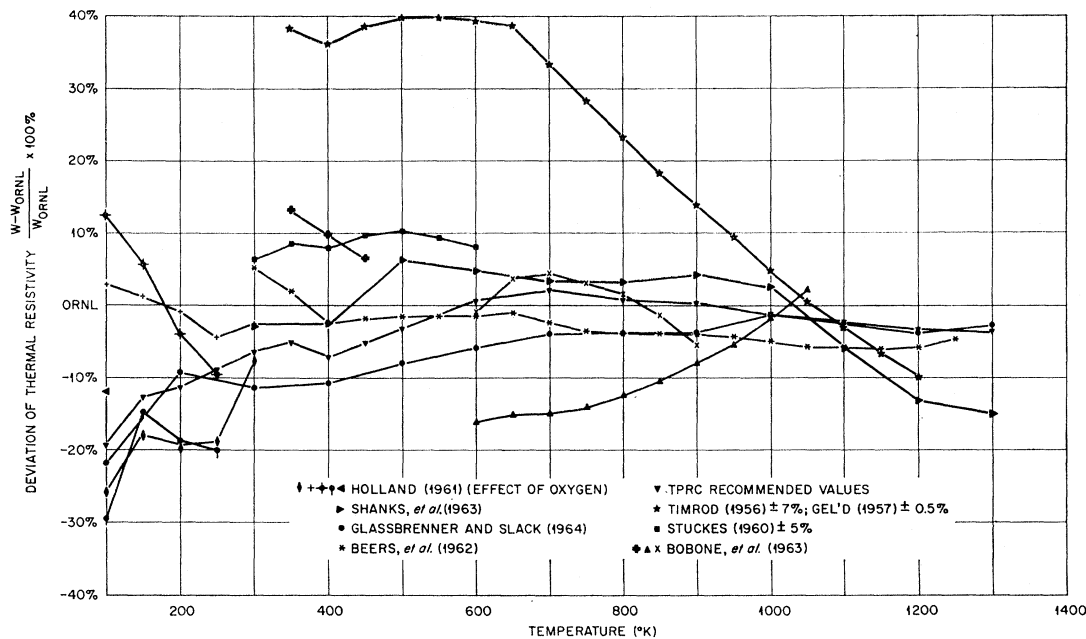


FIG. 7. Difference plot comparing the thermal-resistivity values reported in the literature with those obtained in this work.

ture data of Glassbrenner and Slack have been corroborated. Glassbrenner and Slack's data are consistently below us, amounting to as much as 21% at 100°K, and this difference can probably be attributed to a greater purity and perfection of their samples.

We are in excellent agreement (6% or better) with the data of Beers, Cody, and Abeles²¹ over the entire temperature range of their measurements. The data of these authors for thermal resistivity can be well represented by a linear relation between 300 and 670°K, as can ours. Also, the data for one specimen reported by Holland²² is linear and in essential agreement with our results from room temperature to about 140°K. Holland²² measured the effect of oxygen concentration on the thermal conductivity of silicon which accounts for much of the spread in his data shown in Fig. 7 where each symbol represents a different specimen. The Holland²² data, which agrees with ours, was for a specimen which had a reported oxygen concentration of 7×10^{17} (oxygen atoms)/cm³ or 8 ppm whereas our specimen had 24 ppm oxygen. However, Holland reported that the oxygen content of an *n*-type specimen which he heated for 40 h at 1273°K decreased markedly. The analysis of our specimen is for the as-received condition and since we heated the specimen in vacuum to 1273°K during ρ measurements prior to the k measurements the oxygen content of our specimen could have been lower than 24 ppm.

Figure 8 is a difference plot of the radial-heat-flow data from assemblies 1-4 about the ORNL smoothed thermal-resistivity values. Most of the data lies within

the $\pm 2\%$ most probable error band; however, as we mentioned already the spiral plane data were consistently above the regular plane data whereas the results obtained in assembly 4 for the polycrystal regular plane using (W-5% Re)-(W-26% Re) thermocouples were low. The bulk of the data at the low-temperature end is below the zero line showing a negative deviation from the straight-line fit. This deviation may be due to increased experimental error since the low-temperature data from the radial-heat-flow apparatus was obtained with a small temperature difference of less than 1°K. The discrepancy might also be due to a nonlinear thermal resistance behavior in the 400-500°K temperature range contrary to the linear relation assumed in fitting the data. However, the absolute longitudinal-heat-flow data above 130°K was linear with approximately the same slope as the linear fit through the radial data below 670°K as can be seen by comparing the B constant given in Table V for the average of all the radial-heat-flow measurements below 670°K ($B = 2.954 \times 10^{-3}$ cm/W) with the B constant for the longitudinal-heat-flow measurements between 130 and 350°K ($B = 3.043 \times 10^{-3}$ cm/W). Because of the use of several different thermal-conductivity apparatus we can say only that the thermal resistivity follows a linear relationship between 130 and 670°K to within about $\pm 2\%$.

Figure 8 gives a good picture of the over-all behavior of the radial data but the behavior of each plane is more instructive about the detailed temperature dependence of the thermal resistivity. Table V gives a list of the constants obtained from least-squares fits of the data to linear equations for all the planes individually as well

²² M. G. Holland, in *Proceedings of the International Conference on Semiconductor Physics, Prague, 1960* (Czechoslovak Academy of Sciences, Prague, 1961), p. 633.

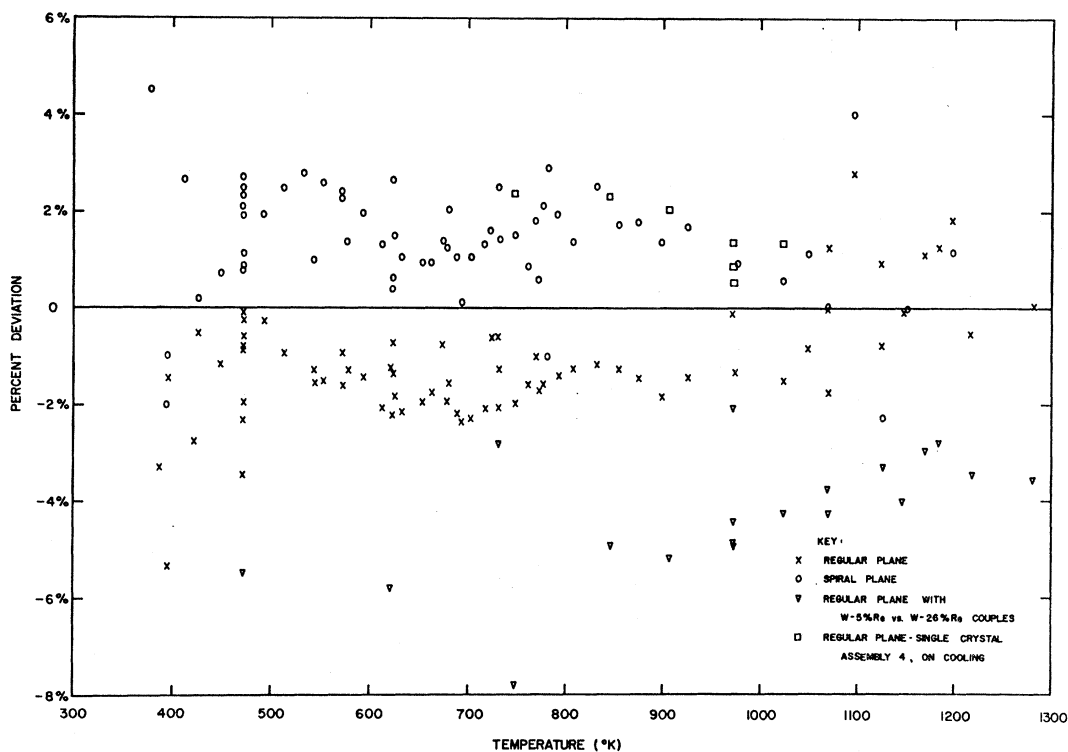


FIG. 8. Deviation of ORNL data points from the smoothed results. Percent deviation equals $[(\text{data} - \text{smoothed}) / \text{smoothed}] \times 100$.

as for combinations of planes. The equation for the low-temperature longitudinal-heat-flow data above 130°K is also included. The standard deviation of the fits shows that the linear relations fit the data very closely between 130 and 1050°K (standard deviation less than 1.25% for individual planes below 670°K and less than 0.7% above 670°K). The agreement between the various planes as to the temperature slope of the thermal resistivity is very good. The lines for the various planes were essentially parallel to each other. The average slope for the individual planes below 670°K was $2.946 \times 10^{-3} \text{ cm/W}$ and the maximum deviation from this average slope was 3%. Above 670°K the average slope was $4.287 \times 10^{-3} \text{ cm/W}$ with a maximum deviation of 4%. This is about a 45% increase in slope.

The data for the single-crystal regular plane instrumented with (Pt-10% Rh)-Pt thermocouples obtained in assembly 4 upon cooling from 1328°K is marked on Fig. 8 with a different symbol. These data were 2-3% higher than those obtained upon heating although the two sets of data were roughly parallel. To check whether this shift was due to thermocouple contamination the stack was reinstrumented again using the same regular planes as for assembly 4 and the data of assembly 5 were obtained. These data showed that the shift in thermal resistivity of the regular single-crystal plane was not due to thermocouples but was apparently due to a specimen change, perhaps oxidation. The change in the thermal resistivity from this effect was about 0.05 cm deg/W . The polycrystalline regular plane, however, showed no

change. This was also indicated by the fact that the (W-5% Re)-(W-26% Re) results of assembly 4 showed no variation on cycling (after the loss of two of the six thermocouples). The results of the assembly 5 measurements lead us to the conclusion that both the types of thermocouples were giving the right temperature dependence for the silicon thermal resistivity during assembly 4. This is very important since the results from both types of thermocouples gave the same magnitude of bend-down at high temperatures showing the same magnitude of electronic contribution to the thermal conductivity as is discussed below.

To test the effects of environment and heat treatment on the thermal conductivity of the silicon, measurements were made in the comparative longitudinal-heat-flow apparatus on a specimen cut from the eighth polycrystalline disk which had not been heated previously. The data are shown in Figs. 4 and 9. It is seen that the thermal conductivity of the specimen did not change on heating in vacuum to 773°K and slow cooling or on heating in vacuum to 773°K and quenching in ice water. For this latter experiment the specimen was sealed in a quartz ampoule containing helium gas and a zirconium getter. The thermal resistivity of the specimen did increase by approximately $0.015\text{--}0.02 \text{ cm } ^\circ\text{K/W}$ on heating in helium in intimate contact with bubbled alumina and fine-grained alumina to 773°K for one week. This last test was meant to simulate the environment of the radial-heat-flow apparatus and shows that the change

TABLE V. Least-squares fits of ORNL thermal-resistivity data for various silicon planes to the relation $A+BT$.

Temperature range	Material	Standard deviation (%)	Constants		
			A (cm deg W ⁻¹)	B (10 ⁻³ cm/W)	
Below 670°K	All planes ^a	1.92	-0.117	2.954	
	All planes ^a plus the absolute longitudinal-heat-flow data above 130°K and including comparative longitudinal-heat-flow data	2.18	-0.198	3.099	
	Regular planes ^a	1.01	-0.121	2.920	
	Spiral planes	1.25	-0.116	2.995	
	Single-crystal regular ^a	1.09	-0.109	2.897	
	Polycrystal regular ^a	0.67	-0.147	2.968	
	Single-crystal spiral	1.10	-0.141	3.040	
	Polycrystal spiral	0.82	-0.056	2.890	
	130-350°K	Polycrystal rod by absolute longitudinal heat flow	0.53	-0.198	3.043
	130-383°K	Polycrystal rod by absolute longitudinal and pellet by comparative longitudinal heat flow	0.83	-0.201	3.056
Above 670°K	All planes ^a	1.58	-0.961	4.229	
	Regular planes ^a	0.50	-0.981	4.212	
	Spiral planes	0.65	-0.957	4.269	
	Single-crystal regular ^a	0.40	-1.088	4.351	
	Polycrystal regular ^a	0.26	-0.913	4.133	
	Single-crystal spiral	0.69	-0.956	4.268	
	Polycrystal spiral (three points)	0.01	-1.047	4.397	
	Polycrystal regular [(W-5% Re)-(W-26% Re)]	0.43	-1.140	4.272	

^a This fit was obtained without including the data obtained in assembly 4 for the polycrystal regular plane using (W-5% Re)-(W-26% Re) or the data from assembly 5.

in resistivity of the regular single-crystal disk in run 4 was probably due to contamination.

Electrical Resistivity and Seebeck Coefficient

Electrical resistivity values were obtained for both the single-crystal and polycrystalline specimen. In the intrinsic range the resistivity of both specimens followed the equation

$$\log_{10}\rho = -4.247 + \frac{2.924 \times 10^3 \text{ }^\circ\text{K}}{T} \quad (\rho \text{ in } \Omega \text{ cm}), \quad (2)$$

at least up to the highest temperature of the measurements which was 1273°K. This result agrees very well (better than $\pm 5\%$) with the data reported by Morin and Maita.³

For both specimens, heating caused shifts in the resistivity in the extrinsic temperature range. This behavior is illustrated in Fig. 10 by the data for the single-crystal specimen. The initial resistivity at room temperature was about 140 Ω cm but after heating to 773°K the room-temperature resistivity was reduced to 50 Ω cm. This behavior continued until after heating to 1260°K the room-temperature resistivity was reduced to 2.5 Ω cm. For the polycrystal specimen the room-temperature resistivity dropped from about 30 to 2 Ω cm upon heating to 1100°K but returned to a higher value of about 15 Ω cm upon heating to 1273°K. All the measurements in the extrinsic range showed

that the resistivity increased with temperature to a maximum just before the specimen became intrinsic.

It should be restated that the low-temperature longitudinal-heat-flow measurements were made on the electrical-resistivity polycrystalline specimen after the electrical-resistivity and Seebeck-coefficient measurements had been completed. It is not known what effect

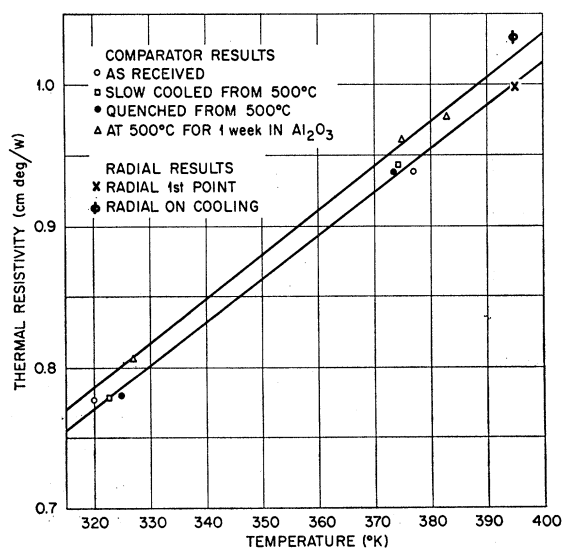


Fig. 9. Thermal-resistivity data obtained in the comparative longitudinal-heat-flow apparatus showing the effect of various heat treatments.

the heat treatment had on the low-temperature thermal conductivity since the specimen was not measured in the as-received condition. Holland²² observed a marked decrease in the oxygen content of an *n*-type specimen which he heat treated for 40 h at 1273°K. The effect of this decrease was to raise the thermal conductivity of this specimen above what it had been prior to heat treatment for temperatures above approximately 20°K. However, Holland did not observe any change in the room-temperature electrical resistivity of his specimen

due to heat treatment. The change of the electrical resistivity of our specimen with heat treatment indicates a change in the electrically active impurities and oxygen is not active according to Holland.²² Changes in ρ of the order of magnitude which we have observed could be produced by changes in electrically active impurity concentrations of much less than 1 ppm.

Both specimens were *n*-type, as revealed by a negative absolute Seebeck coefficient, and both had roughly the same temperature dependence, as shown in Fig. 11,

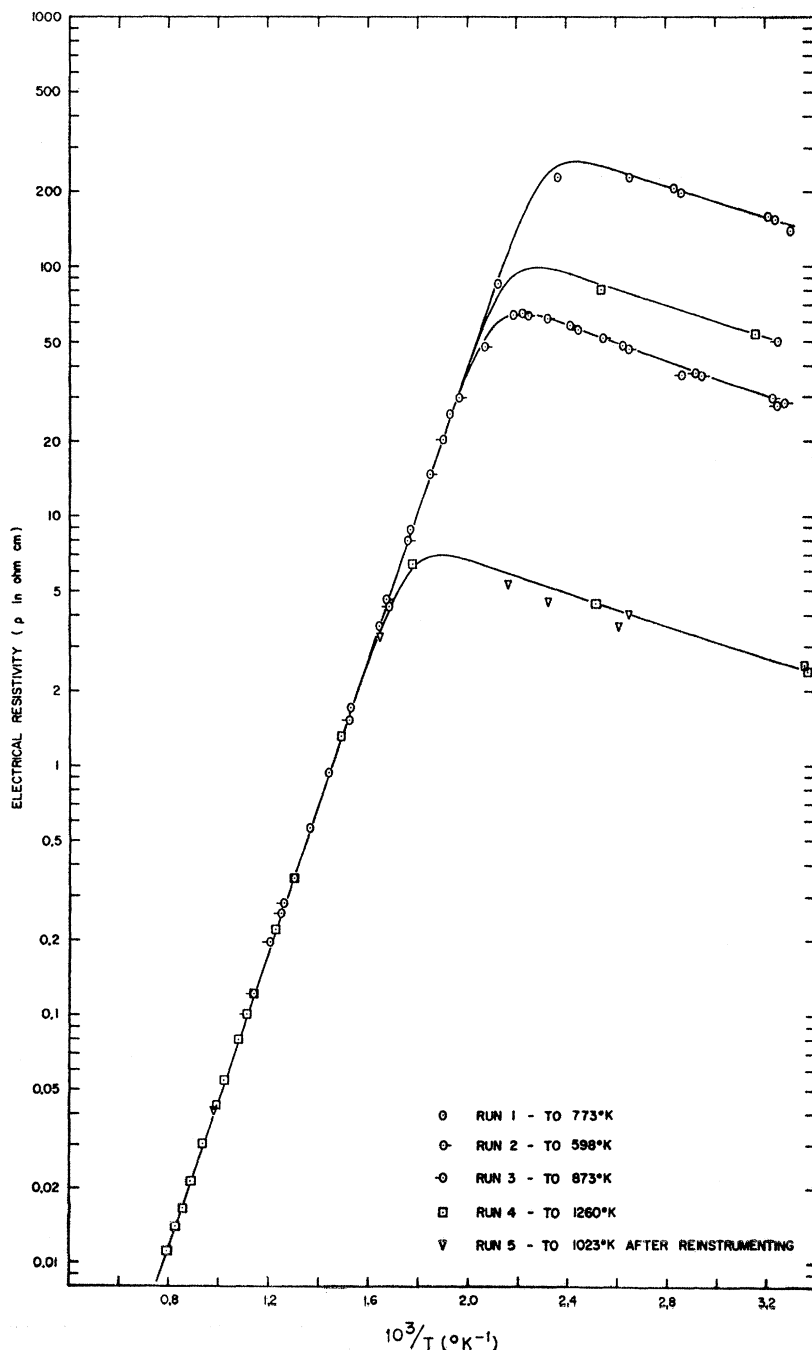


FIG. 10. The electrical resistivity of single-crystal silicon.

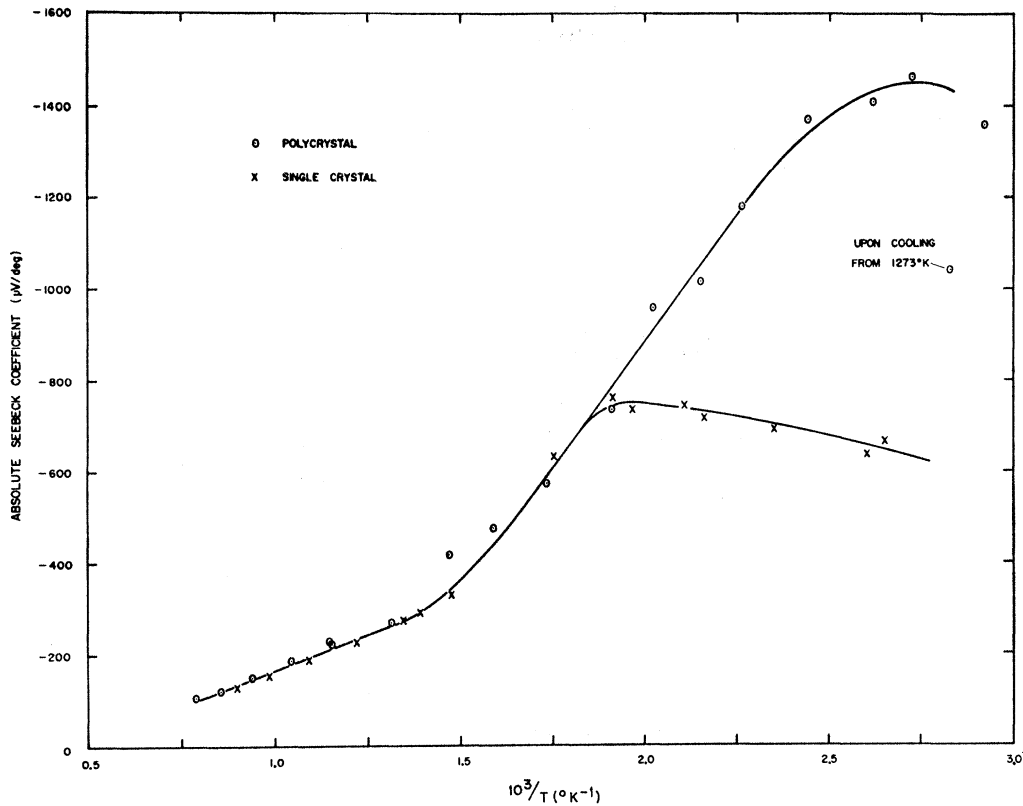


FIG. 11. The absolute Seebeck coefficient of single-crystal and polycrystal silicon.

where the data for the two specimens are plotted versus $1/T$. It is seen that well into the intrinsic range (above 600°K) the Seebeck coefficients become identical and that as the temperature is increased from room temperature the Seebeck coefficient rises to a maximum from which it drops off very rapidly. The dropoff for the single-crystal sample began at about the temperature range of transition between extrinsic and intrinsic of the electrical resistivity but the dropoff began at considerably lower temperatures for the polycrystal specimen. Heating the specimen to 1273°K caused approximately 30% reduction in the value of the Seebeck coefficient of the polycrystal specimen measured at 350°K , whereas heating the single-crystal specimen to 1123°K had negligible effect on the low-temperature coefficient. The temperature dependence of the Seebeck coefficient shown in Fig. 11 is very similar to that obtained for n -type silicon by Geballe and Hull²³ and in the intrinsic region our values agree very well with theirs.

It is most interesting to note that there is a break in the Seebeck-coefficient-versus- $1/T$ plot at a temperature of about 670°K exactly where the break in the thermal-resistivity curve occurs. However, the Hall co-

efficient data of Morin and Maita³ do not show any irregularity at this temperature nor does there appear to be any anomaly in other properties such as specific heat or expansion coefficient.²⁴ The Seebeck break apparently indicates that the material has become entirely intrinsic.²³

DISCUSSION OF THERMAL-RESISTIVITY RESULTS

Assuming that phonons, conduction electrons, and photons each contribute independently to the thermal conductivity, then we may write

$$k = k_L + k_e + k_r, \quad (3)$$

where k_L , k_e , and k_r are the respective contributions. The best estimate¹ for the magnitude of these components is that k_L is at least 95% of the total at temperatures below 1000°K . At the higher temperatures k_e becomes more important with the estimate that at the melting point of silicon it is 30–40% of the total.¹ In the range where k_e is important k_r is expected to be negligible due to the interaction between photons and the current carriers in the material. This expectation is borne out by recent measurements by Ukhanov²⁵ which show that the adsorption coefficient of silicon at a given

²³ T. H. Geballe and G. W. Hull, Phys. Rev. **98**, 940 (1955).

²⁴ *Thermophysical Properties of High Temperature Solid Materials*, edited by Y. S. Toulonkian (The Macmillan Company, New York, 1967), Vol. 1, pp. 878–889.

²⁵ Yu. I. Ukhanov, Fiz. Tverd. Tela **3**, 2105 (1961) [English transl.: Soviet Phys.—Solid State **3**, 1529 (1962)].

TABLE VI. The radiation contribution to the thermal conductivity using the Genzel formula with an integrated average adsorption coefficient and 3.5 as the index of refraction.

Temperature (°K)	$1/\bar{\alpha}$ (cm)	k_r ($\text{W cm}^{-1} \text{ deg}^{-1}$)	k_r/k_{total} (%)
500	0.67	0.031	4.2
550	0.23	0.0141	2.1
600	0.13	0.0103	1.7
700	0.027	0.0034	0.66
800	0.015	0.0028	0.67

wavelength increases rapidly with temperature. On the basis of the Ukhanov data and using the Genzel²⁶ equation for k_r , Glassbrenner and Slack¹ state that k_r is at most 2% of the total. We have repeated their calculation by approximating the Planck distribution with the Wein formula. The results of the calculation are given in Table VI and corroborate the Glassbrenner and Slack statement except at 500°K. However this calculation will not be appropriate when $\bar{\alpha}d \cong 1$, where $\bar{\alpha}$ is the average absorption coefficient and for our case d was taken to be the length corresponding to the difference between the inside radius of the core-heater hole and the radius of the inside thermocouple wells (in the case of the regular planes). For this criterion, below about 500°K silicon is effectively transparent and we can calculate a maximum loss of heat by direct radiation transmission from the core heater through the solid by assuming that the core heater and outside surface of the specimen are blackbodies and that there is no reflection by the alumina granules around the core heater or by the specimen surfaces. This gives a radiation loss of 1.8 and 2% respectively, at 400 and 500°K for the core-heater surface running 20 deg hotter than the specimen. The core-heater temperature was obtained from the resistance of the rod, knowing the resistance as a function of temperature from measurements when the stack was isothermal. This means that below 500°K the thermal resistance data could be at the most 2% below the actual values because of radiation transmission. The effect was probably much less due to scattering of the radiation by the alumina powder around the core heater and by the specimen surfaces.

On the basis of these calculations we will assume for the present that direct radiation transmission and k_r are negligible, bearing in mind that these radiation effects can be of the order of 2% below 600°K. Glassbrenner and Slack¹ have calculated the electronic contribution k_e , including both polar and ambipolar terms, from the equation

$$k_e = 2 \frac{T}{\rho} \left(\frac{k^*}{e} \right)^2 + \frac{b}{(1+b)^2} \left(4 + \frac{E_G}{k^*T} \right)^2 \frac{T}{\rho} \left(\frac{k^*}{e} \right)^2, \quad (4)$$

where k^* is Boltzmann's constant, e is the electronic charge, b is the hole-to-electron mobility ratio and E_G is

²⁶ L. Genzel, *Z. Physik* **135**, 177 (1953).

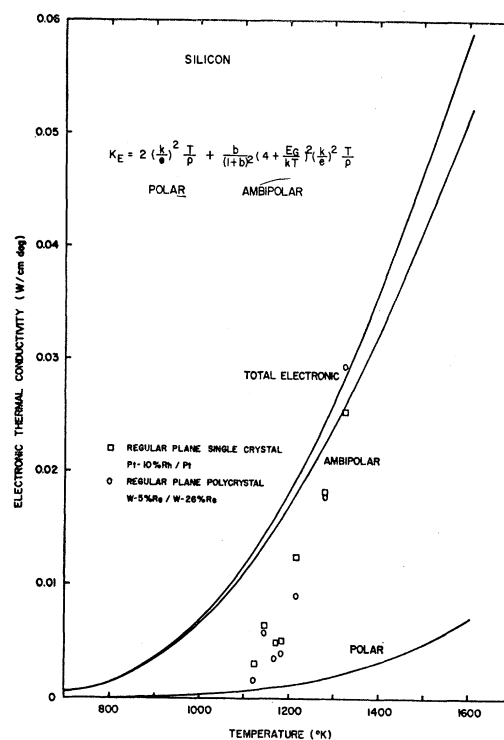


FIG. 12. The electronic contribution k_e for silicon.

the energy-band gap. Figure 12 shows the magnitude of the calculated contributions. The data points plotted in Fig. 12 will be discussed later. It is seen that k_e is less than 1% of k below 900°K but becomes an increasingly important contribution at higher temperatures. Unfortunately, the theory for k_e is not exact, since the electronic band structure of silicon is much more complex than the simple two-parabolic-band model for which Eq. (4) applies. The effect of the complexity on k_e has not been calculated to our knowledge.

In their calculation of k_e Glassbrenner and Slack used the hole-to-electron mobility ratio of about 0.43 obtained from the Hall-coefficient measurements of Morin and Maita.³ This mobility ratio can also be calculated for the intrinsic semiconductor from the Seebeck coefficient. Johnson²⁷ writes the expression for the Seebeck coefficient of an intrinsic semiconductor as

$$Q = - \frac{k}{e} \frac{1-b}{1+2b} \frac{E_0}{2k^*T} + \text{const}, \quad (5)$$

where b is the hole-to-electron mobility ratio, k^* is Boltzmann's constant, e is the magnitude of the electronic charge, and E_0 is the forbidden band gap at 0°K. Thus, Q versus $1/T$ should be a straight line at high temperatures, which is what we find in Fig. 11 for Q

²⁷ V. A. Johnson, in *Progress in Semiconductors*, edited by Allen F. Gibson (John Wiley & Sons, Inc., New York, 1956), Vol. 1, pp. 63-97.

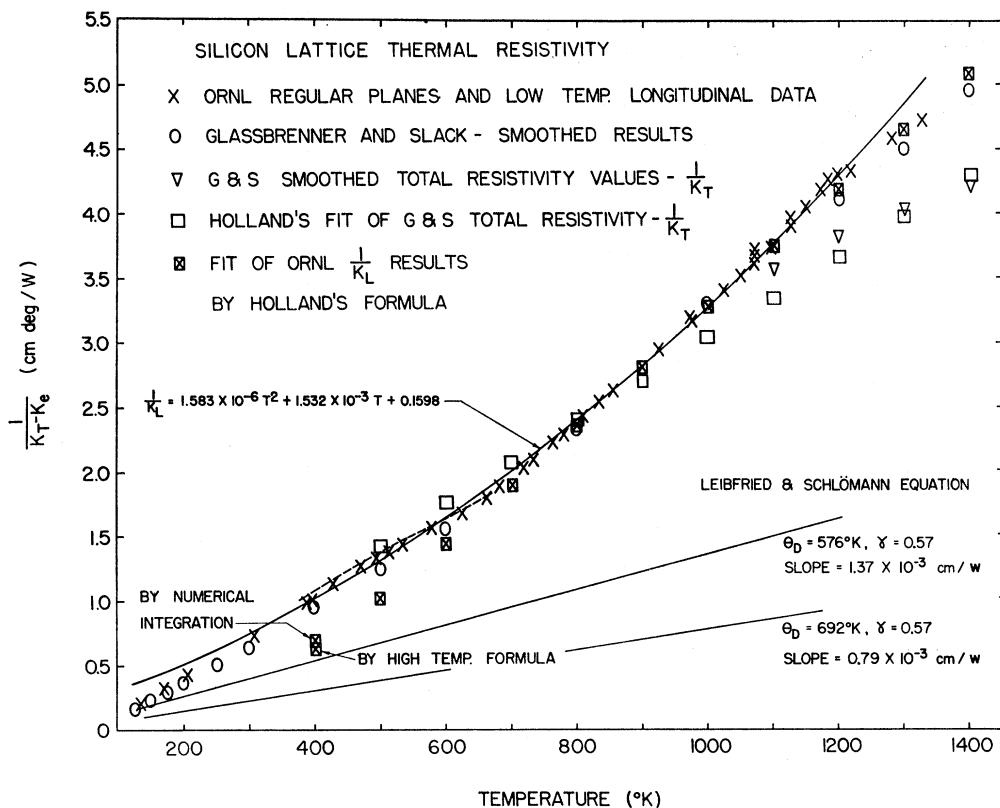


FIG. 13. The lattice thermal resistivity of silicon.

above 670°K, and the slope gives a value of b of 0.31²⁸ using a value of 1.21 eV for E_0 after Morin and Maita.³ This Seebeck value is in reasonably good agreement with the Hall-coefficient determination, and the value of 0.31 would lead to about a 15% reduction in the ambipolar electronic contribution as calculated by Glassbrenner and Slack and shown in Fig. 12.

Despite these uncertainties it is believed that the calculated value of k_e is of the right magnitude. This is also indicated by the data points plotted in Fig. 12 which were obtained by extrapolating the linear relation for the thermal resistivity between 670 and 1050°K to higher temperatures and by assuming that this extrapolation was indicative of the lattice thermal resistivity. The agreement between the results for the two different types of thermocouples is excellent but the value of k_e obtained in this way falls to zero with decreasing temperature much more quickly than indicated by the theory.

²⁸ It is apparent from Fig. 11 that Q versus $1/T$ is approximately linear over a range below 670°K but with a different slope. If we use this slope with Eq. (5) we get a negative b value indicating that the equation does not hold in the lower-temperature region. This lower-temperature range is apparently the range of transition from extrinsic to intrinsic behavior for the Seebeck coefficient and its temperature dependence has been explained quite generally by Geballe and Hull (Ref. 23). It appears to be only fortuitous that this transition is complete at about 670°K—the temperature at which the break occurs in the thermal resistivity. At least, if there is a relation between the two phenomena we are not aware of it.

This may be due to using the wrong value of k_L at high temperatures. For this reason we have reversed our approach and have obtained k_L by subtracting the calculated value of k_e from the total thermal conductivity and have plotted $1/k_L$ thus obtained in Fig. 13.

Since we are interested in the temperature dependence of $1/k_L$, we have plotted only the data for the regular planes using (Pt-10% Rh)-Pt thermocouples and the data obtained from the longitudinal-heat-flow apparatus at lower temperatures. The data should represent the temperature dependence of the lattice thermal resistivity of our specimen very well below 900°K except for a fuzzy region from 400–600°K due to possible 2% radiation transmission and k_r effects. The uncertainty band in the thermal resistivity above 900°K depends on the uncertainty in the calculated k_e .

In the following discussion we compare the temperature dependence of $1/k_L$ as shown by the data points in Fig. 13 to various theoretical predictions. We hoped to find a theory which predicts the temperature dependence of $1/k_L$ so that we would have a firm basis upon which to extrapolate to high temperatures in order to determine k_e experimentally.

The simplest theory would predict that, for $T > \Theta_D$,

$$W = 1/k_L = A + BT, \quad (6)$$

where BT is the thermal resistivity due to three-phonon

umklapp processes and A is a constant term to account for isotope, impurity, and imperfection scattering. The Debye temperature Θ_D is in the range 505–692°K (Gschneidner²⁹ and Herstein³⁰). The magnitude of the isotope resistivity is calculated by Glassbrenner and Slack¹ to be 0.033 cm deg/W. The impurity resistivity, assuming only mass difference scattering and that all the impurities are atomic oxygen, can be calculated from the formula of Ambegaokar³¹ for small impurity concentrations at high temperatures,

$$W_{\text{imp}} = \frac{2\pi^2 c(1-c)(M_2 - M_1)^2}{12\pi \hbar \bar{v}^2 N \bar{M}^2} \Theta_D$$

$$= 5.2 \times 10^{-4} \text{ cm deg/(W ppm)}, \quad (7)$$

where Θ_D is the Debye temperature taken as 670°K, c is the atom fraction of oxygen atoms, M_2 is the atomic weight of oxygen, M_1 is the atomic weight of silicon, \bar{v} is the average velocity of sound (taken as 6.4×10^5 cm/sec after Holland³²), N is the number of atoms/cm³, and \bar{M} is the average atomic weight. Thus, if we have the equivalent of 30-ppm O atom impurities, we might expect a constant thermal resistivity of 0.015 cm deg/W or the same order of magnitude as the isotope term. Therefore, A could be of the order of 0.1 cm deg/W or less. The data of Holland²² show an effect of dissolved oxygen of about 0.0024 cm deg/(W ppm) on the thermal resistance of n -type silicon at 100°K. This is a much larger effect than we have calculated by Eq. (7) and leads us to the conclusion that the impurity-scattering thermal resistivity could be considerably larger than the isotope-resistivity term. This conclusion is also supported by the observed effects of heat treatment on the thermal resistivity which, within the confines of Eq. (6), were described by an increase in A . The difference in thermal resistivity between our measurements and those of Glassbrenner and Slack,¹ who measured on oxygen-free material, varied from 0.02 to 0.06 cm deg/W between 90 and 300°K, the Glassbrenner and Slack resistivity values being lower. This difference is certainly reasonably attributed to specimen impurity differences although one might expect the difference to be a constant.

We have already said that the data for $1/k$, the total thermal resistivity, between 670 and 1050°K are well fitted by a straight line. This is not true for $1/k_L$ plotted in Fig. 13. The data are concave upward from about 900 to about 1200°K above which $1/k_L$ turns back down. Similar behavior is observed for the Glassbrenner and Slack smoothed data shown in Fig. 13 after subtracting k_e . However, a straight line may still be drawn through the data from 670 to 900°K. The problem is that, for

²⁹ Karl A. Gschneidner, in *Solid State Physics*, edited by Frederick Seitz and David Turnbull (Academic Press Inc., New York, 1964), Vol. 16, pp. 275–426.

³⁰ F. H. Herstein, *Advan. Phys.* **10**, 313 (1961).

³¹ V. Ambegaokar, *Phys. Rev.* **114**, 488 (1959).

³² M. G. Holland, *Phys. Rev.* **132**, 2561 (1963).

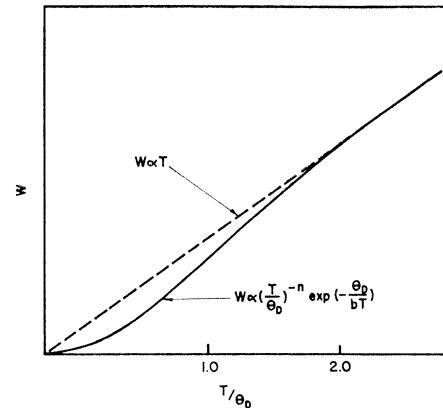


FIG. 14. The qualitative ideal behavior of the lattice thermal resistivity of a pure defect-free infinitely large single-crystal insulator.

this line, the intercept turns out to be negative and of the order of 1 cm deg/W as shown in Table V by the values of A . We can explain this negative intercept for a perfectly pure defect-free insulator as has been proposed by Godfrey *et al.*¹¹ This is illustrated qualitatively in Fig. 14. At very high temperatures ($T \gg \Theta_D$), $1/k_L \propto T$, whereas at very low temperatures ($T \ll \Theta_D$) the thermal resistance should have an exponential form as

$$1/k_L \propto (T/\Theta_D)^{-n} \exp(-\Theta_D/bT), \quad (8)$$

where n and b are constants of the order of unity.³³ Thus, in the temperature range between these extremes ($T \approx \Theta_D$) there must be a gradual transition between the two types of temperature dependence and in this region the intercept of a tangent to the $1/k_L$ curve will be negative. Furthermore, if one were to look at a short temperature span around $T \cong \Theta_D$ the thermal-resistance data would appear linear.

The qualitative behavior of $1/k_L$ plotted in Fig. 13 above 670°K is very similar to that shown in Fig. 14 and our argument is similar to the one used by Shanks *et al.*² The argument also fits the data for BeO reported by Taylor³⁴ which has a linear $1/k_L$ behavior with a negative intercept in the range ($\Theta_D < T < 2\Theta_D$).

What this line of reasoning does not account for is the linear behavior of the data below 670°K, and we

³³ The specific argument used by Godfrey *et al.* (Ref. 11) was wrong due to the fact that Eq. (8) is a low-temperature formula which should not be expected to degenerate into the high-temperature formula. Specifically, the assumption that n can be negative and equal to -1 is not well founded. Nevertheless, the qualitative argument illustrated in Fig. 14 is valid. It is interesting that G. A. Slack and S. Galginitis [*Phys. Rev.* **133**, A253 (1964)] and Glassbrenner and Slack (Ref. 1) use a form for the relaxation time due to three-phonon umklapp processes in Callaway's formulation of the lattice thermal conductivity which is tantamount to assuming $n = -1$ in Eq. (8) and gives the same result of a negative intercept in the limit of $T \gg \Theta_D$. A. F. Joffe [*Physics of Semiconductors* (Academic Press Inc., New York, 1960), p. 280] has also proposed an explanation for the negative intercept which is based on an observation for metals about the mobility dependence on the thermal energy.

³⁴ R. E. Taylor, *J. Am. Ceram. Soc.* **45**, 74 (1962).

consider now the alternative explanation of Glassbrenner and Slack.¹ These authors propose that the linear region below 670°K is the more nearly characteristic of three-phonon resistance (presumably because of the transverse phonon branches with characteristic temperatures well below the specific-heat Debye temperature³²) and that the upswing above 670 is due to four-phonon resistance proportional to T^2 at high temperature. The apparent turnover of $1/k$ above 1200°K is attributed to an underestimate of k_e . If we fit the radial-heat-flow data for the regular planes by a least squares criterion to a quadratic we get the formula

$$1/k_L = 1.583 \times 10^{-6} T^2 + 1.532 \times 10^{-3} T + 0.1598. \quad (9)$$

This is very close to the equation obtained by Glassbrenner and Slack,¹

$$1/k_L = 1.65 \times 10^{-6} T^2 + 1.56 \times 10^{-3} T + 0.03,$$

except for the intercept. The low-temperature longitudinal-heat-flow data falls below the extrapolation of this formula but the formula is not expected to hold at low temperatures and the deviation can be explained by the same sort of negative intercept argument used above only shifted to lower temperature. The constant intercept is the right order of magnitude for the resistivity due to isotope-plus-impurity scattering. The coefficient of T is also the right order of magnitude for three-phonon processes calculated using the equation derived by Leibfried and Schlömann³⁵ and modified for the deviation of the Grüneisen constant γ from 2.0 after Steigmeier and Kudman³⁶ by multiplying by

$$(1 + 1/2\gamma)^2.$$

Using a value²⁹ of γ of 0.57 and a minimum and maximum value²⁹ of Θ_D of 576 and 692°K, respectively, one obtains values of $1.37 \times 10^{-3} T$ and $0.79 \times 10^{-3} T$ for the three-phonon thermal resistivity and these lines are plotted in Fig. 13.

The main difficulty with this fit of the data is that all of the data from 600–800°K lie below the calculated curve. This can hardly be called a random disagreement between experiment and theory. This disagreement is of the order of magnitude to be explained by a radiation contribution since it is about 2%. However, our calculations of this component given in Table VI lead to a shift of $1/k_L$ to the dotted line in Fig. 13 which does not help because the radiation correction does not have the right temperature dependence. The estimate below 500°K is based on a 2% maximum radiation transmission of the core-heater power.

It should be mentioned that an added component for $1/k_L$ beyond the $A + BT$ terms is expected from several

other sources besides four-phonon processes. First of all, the expansion of the lattice causes a decrease in the Debye temperature which would lead to a T^2 increase in $1/k_L$ if Θ_D were assumed to be a linear function of T . Secondly, Ranninger³⁷ has recently analyzed the lattice conductivity by use of correlation-function techniques rather than by the Boltzmann transport equations and concludes that there will be a T^2 resistance term due to the temperature dependence of the phonon frequency spectrum.

There thus appear to be ample theoretical reasons for expecting the thermal resistivity to increase faster than linearly at high temperature. However, for silicon the total temperature range of the measurements is from $0.15 < T/\Theta_D < 1.98$ assuming Θ_D is 670°K. Of this range the upper temperature limit where one can consider k_e negligible is about 1000°K or $T = 1.5\Theta_D$. The melting point itself is only $2.5\Theta_D$. Thus scaled by Θ_D we are looking at a very small temperature range for this material. Using Eq. (9) we would calculate that the T^2 term is already 30% of the total thermal resistivity at 500°K which is only $0.75\Theta_D$. At $2\Theta_D$ the T^2 term is 55% of the total. It seems to us that this is a very large effect especially when one looks at the data of an insulator like UO_2 where the thermal resistance is given with great precision by a linear formula,¹¹ with a positive intercept from $2.4 < T/\Theta_D < 6.9$ with $\Theta_D = 200^\circ\text{K}$. Thus for UO_2 over a much broader range of T/Θ_D no significant T^2 resistance term appears. This needs to be explained.

It might be that the break at 670°K is due to the sudden onset of an additional scattering of acoustical phonons by optical phonons. Evidence for this scattering mechanism in III-V semiconductors is given by Steigmeier and Kudman.³⁶ However, the evidence also indicates that the effect is already important at the Debye temperature but we would have to argue for silicon that this scattering mechanism becomes important only above the Debye temperature and furthermore that it is a linear addition to the thermal resistance.

Finally we should consider the approach of Holland,³² who fit the data for silicon to phenomenological equations of the form proposed by Callaway³⁸ but accounting specifically for the dispersion of the phonon spectrum of silicon and for the transverse and longitudinal branches of the spectrum. At high temperatures he concludes that the Callaway-type integrals should reduce to the form

$$k_L = A/T - B/T^2 + C/T^3, \quad (10)$$

where the first two terms correspond to the thermal conductivity of the transverse phonons with umklapp processes taken into account and the third term accounts for the thermal conductivity of longitudinal phonons.

Holland assumed that at 1000°K only the first two

³⁵ G. Leibfried and E. Schlömann, *Akad. Wiss. Gottingen Mat.-Physik Kl.* 2A, 71 (1954) (English translation obtainable from Technical Library Research Service, Purchase Order No. B4B-60150, Letter Release No. S-70).

³⁶ E. F. Steigmeier and I. Kudman, *Phys. Rev.* 132, 508 (1963).

³⁷ Julius Ranninger, *Phys. Rev.* 140, A2031 (1965).

³⁸ J. Callaway, *Phys. Rev.* 113, 1046 (1959).

terms were important so he set these equal to the reported value of Glassbrenner and Slack¹ at this temperature. The constants A and B are related so a single value of k_L was sufficient to establish both. He then determined the value C by using the measured value of k_L at 300°K. We have calculated k_L using Holland's prescription and constants³⁹ and these values are indicated on Fig. 13. The numerical values of A , B , and C are 3.29×10^2 W/cm, 0.971×10^4 W deg/cm, and 1.025×10^7 W deg²/cm, respectively. Also shown on the figure for comparison are Glassbrenner and Slack's total thermal-resistivity values (without subtracting the electronic thermal conductivity). Holland's values are reasonably close to these data, as they should be, being tied down at two points. Actually, the tie down at 1000°K is 6% low which is the magnitude of the third term in Eq. (10) at this temperature. The calculated curve is concave downward and therefore does not explain the temperature dependence in the vicinity of 670°K.

We have reapplied the model to our data for k_L with the electronic portion subtracted. We have done this by using 1300 and 900°K as tie-down points to fix A , B , and C which become 2.465×10^2 W/cm, 0.549×10^4 W deg/cm, and 6.32×10^7 W deg²/cm, respectively. The calculated values are plotted in Fig. 13 and these fit the data well down to 700°K where they rapidly diverge from the experimental results. Two calculated points are plotted at 400°K, one calculated by Eq. (10) and the other obtained by actual numerical integration. The two values agree well enough to indicate that the high-temperature formula is an adequate approximation to the integrals down to this temperature.

It should be pointed out that all three terms in Eq. (10) are necessary to account for the negative intercept of a tangent to a curve through the experimental data above 700°K. A tangent to any curve given by the first two terms of Eq. (10) alone will always have a positive intercept. It is for this reason that we choose to iterate between two high-temperature points to find the values for A , B , and C . Thus the Holland treatment as we have modified it appears to fail at low temperatures.

One further scattering mechanism for phonons is by the current carriers. This has been found to be important for heavily doped Ge-Si alloys⁴⁰ and the data for these

alloys have been fitted very closely by Steigmeier and Abeles⁴¹ using Callaway's³⁸ formulation and introducing electron-phonon scattering. Beers *et al.*²¹ suggest that part of the increase in the thermal resistance of silicon at high temperatures is due to electron-phonon scattering. Holland's³² treatment for silicon should be extended to include this possibility as well as the effect of the scattering of acoustical phonons by optical phonons, but it is beyond the scope of this paper to make this extension.

CONCLUSIONS

(1) We have measured the thermal conductivity of pure single-crystal and large-grained polycrystalline specimens of silicon from 90–1328°K and our high-temperature results corroborate the behavior reported by Glassbrenner and Slack¹ but not the results of Shanks *et al.*² The data indicate that the electronic portion of the thermal conductivity is close to that predicted by theory for ambipolar diffusion. The total thermal resistivity can be represented empirically with a straight line from 130–670°K (Θ_D approximately 670°K) and by another straight line with a greater slope from 670–1050°K. Above 1050°K the electronic contribution causes the data to bend downward away from the straight line. We have not been able to theoretically explain all the details of the temperature dependence of the thermal resistivity and therefore we cannot quantify the electronic contribution unambiguously. The major difficulty is a relatively sharp break in the thermal-resistivity-versus-temperature curve at 670°K.

(2) The electrical-resistivity values obtained on intrinsic silicon measured on both single-crystal and polycrystal specimens corroborate the results of Morin and Maita³ to better than 5%.

(3) The value for the mobility ratio calculated from the Seebeck-coefficient data above 670°K is 25% lower than the value obtained by Morin and Maita³ from Hall-coefficient measurements. It is interesting that the Seebeck coefficient plotted versus $1/T$ shows a break at about 670°K where the thermal-resistivity curve also changes slope but it is not thought that these two phenomena are related.

ACKNOWLEDGMENT

The authors would like to express their appreciation to N. D. Woodall, who made many of the electrical-resistivity and Seebeck-coefficient measurements.

³⁹ There seems to be a misprint for the value of the constant related to isotope scattering which Holland calls A . The value should be 1.145×10^{-45} sec³ instead of 1.32×10^{-44} sec³.

⁴⁰ B. Abeles and R. Cohen, *J. Appl. Phys.* **35**, 247 (1964).

⁴¹ E. F. Steigmeier and B. Abeles, *Phys. Rev.* **136**, A1149 (1964).